

Available online at www.sciencedirect.com**ScienceDirect**

Procedia Engineering 145 (2016) 1036 – 1043

**Procedia
Engineering**www.elsevier.com/locate/procedia

International Conference on Sustainable Design, Engineering and Construction

Determining and Validating Thermal Strain in Asphalt Concrete

Mohammad Hossain^{a*}, Mir Azam^b, Rohit Mehta^b, Naushad Shaik^c, Md R. Islam^d,
M.ASCE, Rafiqul Tarefder^e, M.ASCE,

^aAssistant Professor, Civil Engineering and Construction Department, Bradley University, 1501 W Bradley Ave, Peoria, IL, 61625, USA

^bFormer Graduate Student, Mechanical Engineering Department, Bradley University, 1501 W Bradley Ave, Peoria, IL, 61625, USA

^cGraduate Student, Civil Engineering and Construction Department, Bradley University, 1501 W Bradley Ave, Peoria, IL, 61625, USA

^dAssistant Professor, Civil Engineering Technology, Colorado State University-Pueblo, 2200 Bonforte Blv, Pueblo, CO, 81001, USA

^eProfessor, Civil Engineering Department, The University of New Mexico, MSC01 1070, Albuquerque, NM, 87131, USA

Abstract

Thermal strain causes transverse cracks in Asphalt Concrete (AC) pavements. In this study, thermal strain is determined by developing a three-dimensional Finite Element Method (FEM) model and validates the model with measured data using the field installed Horizontal Asphalt Strain Gauge (HASG) in Interstate 40 (I-40) located near the city of Albuquerque in the state of New Mexico. Materials' properties of the pavement section were determined by laboratory testing on field collected cores from the pavement section after the construction. Viscoelastic material properties of AC were determined from the creep test on the field cored samples. Coefficient of thermal expansion (CTE) and contraction (CTC) of AC were also determined in the laboratory and in the field. Results show that the FEM model can predict thermal strain with maximum variation of 6.0% compared to measured thermal strain in the field, which is very promising.

Keywords: Asphalt concrete; Thermal strain; Thermal expansion; Thermal contraction; Finite element model; Field measurement

1. Introduction

Pavement experiences both load and temperature induced strains. Repeated traffic wheel causes load induced strains at the bottom of asphalt layer and temperature variation causes thermal strains throughout the whole layer.

* Corresponding author, Tel: +1-309-677-2945; fax: +1-309-677-2867.

E-mail address: mihossain@fsmail.bradley.edu

Temperature load varies in a day (i.e. hot at day time and cold at night time) and in a year (i.e. hot in summer and cold in winter) [1]. In addition, temperature distribution varies throughout the thickness of pavement structures; such as at day time the top of pavement is warm and the bottom of the pavement is relatively cold and at night time the top of the pavement is colder compare to the bottom of the pavement [2]. This phenomenon is true for both Asphalt Concrete (AC) or flexible pavements and Portland Cement Concrete (PCC) or rigid pavements [2,3]. For this reason, fatigue thermal load has equal importance as fatigue traffic load.

At low temperature, thermal strains cause thermal cracks in AC pavements when thermally induced strains produce localized stresses, which exceed the fracture strength of the materials [4]. In winter, the top of a pavement is colder than the bottom and the thermal strain is critical at the top and for this reason cracks initiate at top of a pavement. Although there are other reasons for transverse cracks such as hardening of asphalt, which is the result of aging of asphalt, and expansion and contraction of underlying PCC pavement joints if AC overlay is used on top of PCC pavements. Several studies have been done on understanding transverse cracks due to low temperature [4]. The referred studies consider asphalt mixture mechanical and thermo-mechanical properties, such as the creep compliance mastercurve, mixture tensile strength, thermal coefficient of contraction, pavement structure, and hourly pavement temperature as a function of depth.

On the other hand, at high temperature, thermal strains coupled with traffic loads cause rutting or permanent deformation in AC pavements [4]. At higher temperature, the AC pavement material becomes nonlinear and applied traffic load causes shear deformation into the pavement leading to permanent deformation. Although there are other reasons for rutting such as excessive asphalt binder in the mix and high voids in the Hot-mix Asphalt (HMA). Rutting appears as longitudinal depression in the wheel paths accompanied by small upheavals to the sides. The width and depth of the rutting is highly dependent upon the pavement structure (i.e. layer thicknesses and material properties), traffic volume and distribution, and site environmental conditions. Several studies have been done on understanding rutting due to high temperature [4].

In real field, temperature varies throughout the day and at some part of the day the pavement experiences contraction due to low temperature and some part of the day the pavement experiences expansion due to high temperature. This study attempts to predict the thermal strain variation in the AC pavement due to change in temperature. Until recently, very few studies have been conducted on determining thermal stain in pavements [5,6]. Previous studies do not separate thermal strains from the total strains and consider it as a conjugate part of strains. However, a detail understanding of thermal strains helps to understand the individual impact of it over elastic and plastic strains of the materials. Indeed, it is very important to study temperature effects in pavements for sustainable design and construction of AC pavements. This is why, the authors have been motivated to study thermal strain in asphalt pavement. This study attempts to use Finite Element Method (FEM) to determine the thermal strain. It also validates the results with field measured data.

2. Objective and scope

The objective of this study is to predict thermal strains in an AC pavement and validate the thermal strains value with the data measured in the field. To fulfill the objective of this study, a three-dimensional FEM model is developed using commercially available software ABAQUS. The FEM model considers viscoelastic material properties as a function of temperature. The predicted thermal strain is validated with the thermal strain measured in Interstate 40 (I-40) located near the city of Albuquerque, New Mexico, USA. Strain gauges have been installed in I-40 interstate to measure total strain, which combines thermal strain and strain due to traffic load. Thermal strain is calculated from the total strain measured by strain gauges and then compared with the thermal strain predicted by the FEM model.

3. Literature

3.1. Measuring thermal strain in field

Thermal strain data was collected from an instrumented pavement section on I-40 in NM. The longitudinal profile of the instrumented section is shown in Fig. 1. The section has four layers. The top layer is a 263 mm thick

HMA layer followed by a 150 mm thick crushed stone base course. There is also a 200 mm thick subbase layer known as Process Place and Compact (PPC). Fig. 1 shows the two HASGs at 90 mm depth and twelve (4 x 3) HASGs at 263 mm depth. It also shows the three temperature probes used to monitor the temperature variations, one at the top of pavement and two at the HASG’s elevation. The centreline of the sensors is 90 mm from the right edge of the driving lane. The three sensors at each row at 263 mm depth are 50 mm apart in the transverse direction. The section also has Vertical Asphalt Strain Gages (VASGs), Earth Pressure Cells (EPCs), moisture probes, Axle Sensing Strips (ASSs), a weather station and a Weigh-in-Motion (WIM) station. The sensor layouts are not presented in Fig. 1 as the data for the sensors are beyond the scope of this study.

Twelve HASGs were installed below the HMA (on top of base layer) at a depth of 263 mm. The sensors were arranged in an array of 4x3. The middle two rows were installed in a transverse direction. Two HASGs (one in transverse and one in longitudinal direction) were embedded on the top of the 2nd lift of the HMA at a depth of 90 mm. Both types of gages are identical. The gauge has two steel arms and two steel legs (“H” shape) and a spring embedded inside a membrane at the centre of the sensor. When surrounding material pushed the two legs, the AC material between the steel legs was squeezed or shortened, and the resulting deformation was measured by the sensor spring inside the membrane. An electric signal was then sent to the data acquisition system, which reported the change in length in terms of voltage. The voltage value was then multiplied by the calibration factor to report the deformation in strain. Temperature probes were bundled together and inserted into a drilled hole. Prior to the inserting, asphalt cement was applied around the probes. The asphalt cement had the same thermodynamic properties of HMA, therefore, no calibration was for asphalt cement. A precise data acquisition system was used which can separate the thermal strain and traffic induced strain.

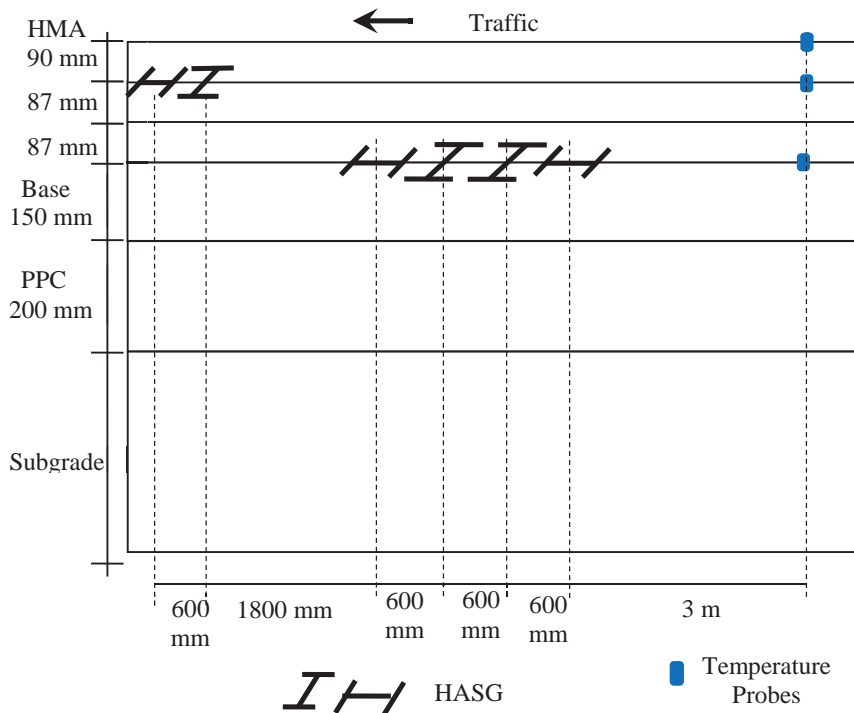


Fig. 1. Longitudinal profile of the instrumented section.

3.2. Thermal conductivity of HMA

Thermal conductivity, k measures the heat flux flowing through a material at unit temperature gradient and is expressed in $W/(m \cdot ^\circ C)$. Islam and Tarefder [6] determined the thermal conductivity (k) of asphalt concrete in laboratory and by developing FEM. Thermal gradient was applied at one end of a cylindrical sample in the laboratory as shown in Fig. 2. Increase in temperature with time at the colder end of the sample was recorded. Based on the laboratory determined specific heat capacity (C) value a FEM model was developed in a commercial FEM software, ANSYS for the cylindrical sample and k value is assigned on trial and error basis. The increase in temperature at the colder end of the model sample was compared with the increase in temperature of the laboratory sample to determine the optimum k value. Using k and C values in FEM, field HMA temperatures at 90 mm depth were predicted from morning to afternoon and compared with measured values. This study determines k value of $2.11 W/(m \cdot ^\circ C)$ for HMA. This value is close to the k value determined by other researchers [7].

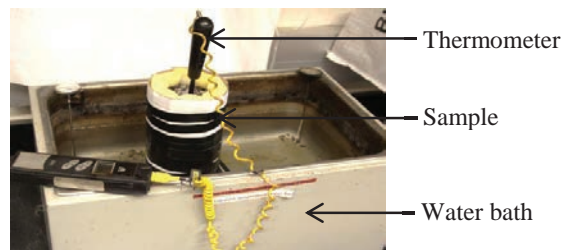


Fig. 2. Applying temperature differential in asphalt sample [6].

4. FEM analysis

4.1. FEM model development

A solid homogeneous three-dimensional FEM model was developed using commercial software ABAQUS to simulate the thermal effect. The FEM model is shown in Fig. 3. The FEM model is of 610 mm long, 610 mm wide and 1220 mm deep. The model consists of 263 mm HMA at the top, 150 mm base beneath the HMA, 200 mm subbase and the subgrade. The HMA layer was separated in three layers since the original pavement is constructed in three lifts. The three HMA layers are named as HMA-1, HMA-2, and HMA-3 with 90 mm, 87 mm, and 87 mm depth.

Fine mesh was assigned near the corner of the FEM model to capture the precise temperature and strain variations in that region. Standard linear element, C3D8 without reduced integration, was used for all section in the pavement structures. The bottom of this model was restrained to move along both the horizontal and the vertical directions and vertical planes were not allowed to move along the horizontal direction. Pavement surface deflects vertically for the truckload and hence, vertical planes are free to move in the vertical direction. In addition, no slip was allowed between the two adjacent layers.

4.2. Material properties for the FEM

To determine the input parameters for the FEM laboratory tests were conducted on asphalt samples. A number of cylindrical samples of 150 mm diameter were collected from a pavement section of I-40 near the instrumented section. The samples were then cut into 50 mm thick circular specimens using laboratory saw. The air voids of the samples ranged between 5.2% and 5.8% with an average value of 5.4%. A dense graded Superpave (SP) mix, type SP-III was used in this pavement section. The design binder was a Performance Grade (PG) PG 76-22 with an asphalt content of 4.4% by the weight of the mixture. The maximum aggregate size was 19 mm. About 5% of the materials passed through a number 200 sieve (0.075 mm).

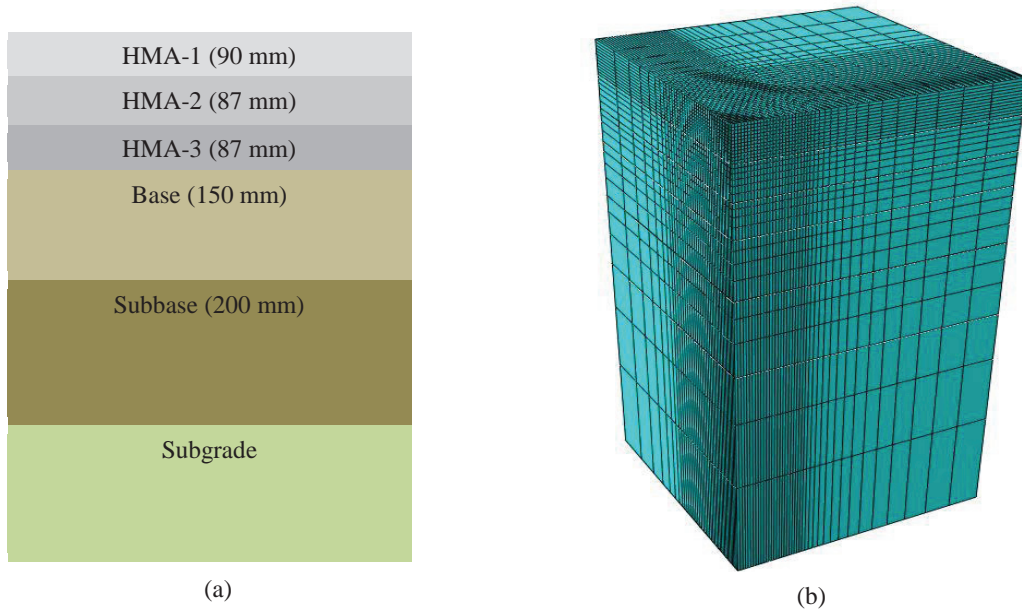


Fig. 3. (a) Pavement layers and (b) FEM model

The creep tests were conducted by applying vertical stress diametrically on asphalt samples. The stress value was selected to keep the strain in the linear viscoelastic range of AC [8]. More detail on the creep test can be found in the referred work. The creep compliance (i.e. $D(t)$) and stiffness (i.e. $E(t)$) are determined as a function of time. The time and creep compliance data are then plotted and the equation (1) is fitted to determine the viscoelastic material properties.

$$D(t) = \frac{1}{E_0} \left(1 + \frac{t}{T_0} \right) + \frac{1}{E_1} \left[1 - \exp \left(-\frac{t}{T_1} \right) \right] \tag{1}$$

where, E_0 is the instantaneous modulus, E_1 is the long-term modulus, T_0 is the relaxation time, and T_1 is the retardation time, and t is the time. After that, the bulk modulus and shear modulus are determined using the equations (2) and (3). The ν_0 is the Poisson's ratio and assumed as 0.35 for HMA.

$$K(t) = \frac{E(t)}{3(1-2\nu_0)} \tag{2}$$

$$G(t) = \frac{E(t)}{2(1+\nu_0)} \tag{3}$$

where, $K(t)$ is the bulk modulus and $G(t)$ is the shear modulus as a function of time. Both bulk and shear modulus are then plotted with time and the equations (4) and (5) are fitted to determine the Prony series parameters, which are the input in the FEM model.

$$K(t) = K_0 \left[1 - \sum_{k=1}^N \bar{k}_k^p \left(1 - \exp \left(-\frac{t}{\tau_k} \right) \right) \right] \tag{4}$$

$$G(t) = G_0 \left[1 - \sum_{k=1}^N \bar{g}_k^p \left(1 - \exp \left(-\frac{t}{\tau_k} \right) \right) \right] \tag{5}$$

where, G_0 is initial shear modulus and K_0 is initial bulk modulus, t is time, and Prony series parameters are \bar{g}_k^P , \bar{k}_k^P , and τ_k and they are determined by fitting the above two equations with the laboratory data. For each temperature N is 3 since that gives best fitting of the laboratory test data. The Prony series values those are calculated using equations (4) and (5) are given in Table (1).

Table 1. Calculated Prony series values used in the FEM model.

Viscoelastic model parameters	N_1	N_2	N_3
g_k^P	0.2077	0.4138	0.2742
k_k^P	0.2114	0.414	0.2712
τ_k	5.694	24.045	116.7

The material properties those are used for HMA, base, subbase, and subgrade are given in Tables (2) and (3). HMA layer was modeled as temperature dependent layer; the modulus of elasticity varies with temperature and the variation is given in table (3). The base, subbase, and subgrade layers were considered elastic.

Table 2. Pavement layers’ material properties used in the FEM model.

Material	Modulus of elasticity (MPa)	Density (kg/m ³)	Poisson’s ratio
HMA	Temp dependent data	2308.74	0.35
Base	590	2159.93	0.45
Subbase	650	1919.97	0.45
Subgrade	160	1759.95	0.40

Table 3. Temperature dependent modulus of elasticity data for the HMA layer.

Modulus of elasticity of HMA (MPa)	Temp (°C)	Modulus of elasticity of HMA (MPa)	Temp (°C)
158.28	-1.50	153.53	-0.18
157.60	-1.31	152.86	0.00
156.92	-1.12	152.19	0.20
156.24	-0.93	151.52	0.39
155.56	-0.74	151.36	0.43
154.88	-0.56	150.85	0.58
154.80	-0.53	150.18	0.77

The thermal property that is used in the FEM model is given in Table (4). These properties are used in the asphalt layer as well as for the other layers. The temperature variations in underneath base/subbase layers are very small and can be reasonable neglected [1].

Table 4. Thermal properties used in the FEM model.

Thermal parameters	Values
Thermal Conductivity	2.11 W/m-°C
Expansion/Contraction Coefficient	2.64E-5 /°C
Specific heat	1463.02 J/Kg-°C

4.3. Thermal loading

The thermal load varies with time of the day in all the layers. Thermal load variation was different within the HMA layer at different depths. All the temperatures were measured by temperature probes installed in the different layers of the pavement. The daily temperature trend of October 26, 2012 in all the layers were used as follows which was measured and showed in Fig. 4. HMA-1 refers temperature measurement at top of pavement, HMA-2 refers temperature measurement at 90 mm depth of pavement, and HMA-3 refers temperature measurement at 263 mm depth of pavement.

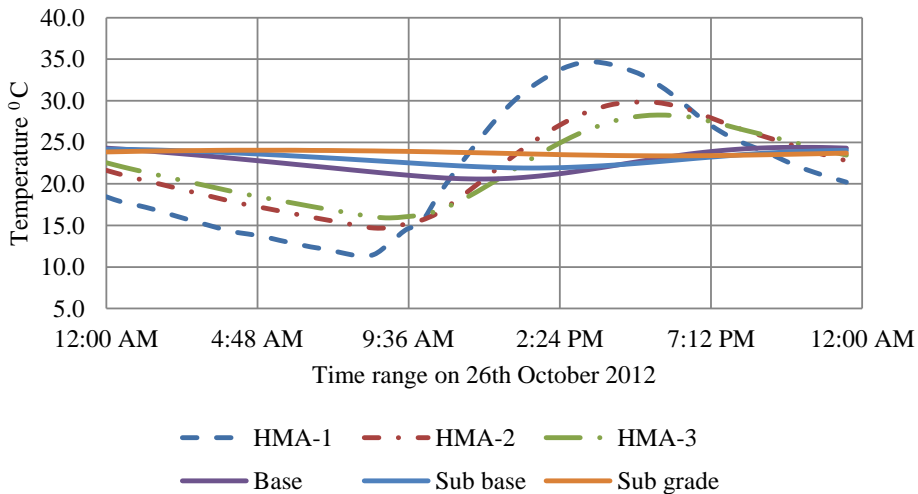


Fig. 4. Temperature variation measured by thermal probe that is used as FEM input

5. Results and Discussion

Fig. 5 shows the horizontal thermal strain variation predicted by FEM model at the bottom of HMA layer and the field measured data. The strain at 12 am (midnight) is considered zero to present the responses. Fig. 5 shows that the thermal strain increases over time and reaches to its peak and then decreases and then and trend shows that the cycle continues with time. The negative strain represents contraction and the positive strain represents expansion of the HMA layer. Clearly, the FEM predicted strain and field measured strain matches closely each other. The maximum deviation between them is 6.0% which can be neglected.

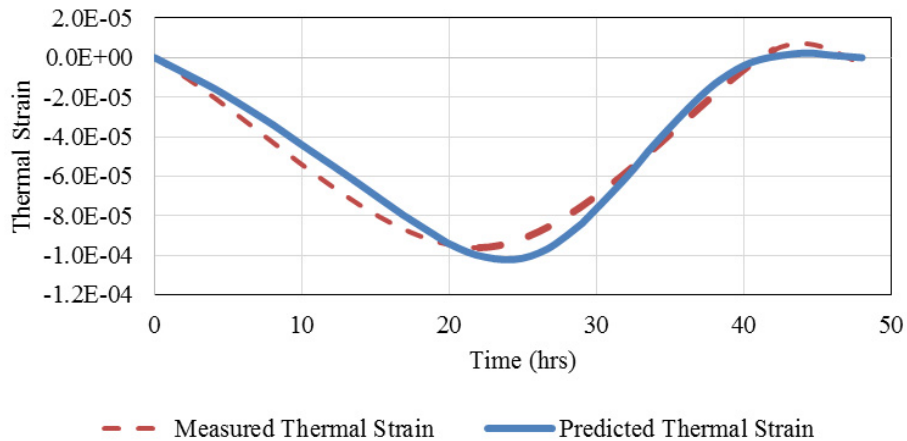


Fig. 5. Predicted and measured thermal strains at the bottom of HMA

6. Conclusions

This study determines the thermal strain of AC using FEM and validates the FEM determined thermal strain by field measurement. This particular AC pavement in NM is instrumented with strain gauges and thermal probes and the temperature reading and strain were measured in the field. Later viscoelastic and thermal properties of the HMA mix of the same pavement structure were determined in the lab. Using these material properties as an input a FEM model the thermal strain was determined. Though the FEM prediction shows good prediction compared to the measured values, the computation time is very long. Parallel computing with high performance computer can be used in future to do future study on similar areas.

Acknowledgements

The FEM modeling study is funded by Center for Teaching Excellence and Learning (CTEL) through Special Emphasis (SE) grant and Caterpillar Fellowship of Bradley University.

References

- [1] Tarefder RA, Islam MR. Study and Evaluation of Materials Response in Hot Mix Asphalt Based on Field Instrumentation Phase I: Final report. Albuquerque, New Mexico, USA: 2015.
- [2] Rao S, Darter M, Tompkins D, Vancura M, Khazanovch L, Signore J, et al. Composite Pavement Systems-Volume 1: HMA/PCC Composite Pavements. Washington, D.C., USA: 2013.
- [3] Rao S, Darter M, Tompkins D, Vancura M, Khazanovich L, Signore J, et al. Composite Pavement Systems-Volume 2: PCC/PCC Composite Pavements. Washington, D.C., USA: 2013.
- [4] Y. Richard Kim, editor. Modeling of Asphalt Concrete. ASCE Press and McGrawHill; 2009.
- [5] Islam MR, Tarefder RA. Determining Coefficients of Thermal Contraction and Expansion of Asphalt Concrete Using Horizontal Asphalt Strain Gage. *Adv. Civ. Eng. Mater.*, 2014, Vol. 3, pp. 204–219.
- [6] Islam MR, Tarefder RA. Determining Thermal Properties of Asphalt Concrete using Field Data and Laboratory Testing. *Constr Build Mater* 2014;67:297–306.
- [7] Luca J, Mrawira D. New Measurement of Thermal Properties of Superpave Asphalt Concrete. *J. Mater. Civ. Eng.*, 2005;17:72–9.
- [8] Islam, M. R., Faisal H. and Tarefder, R. A. (2015). “Determining Temperature and Time Dependent Poisson’s Ratio of Asphalt Concrete using Indirect Tension Test.” *Journal of Fuel*, Vol. 146, pp. 119-124.